

Modeling of the nonlinear interface in reinforced concrete

J. L. Curiel Sosa^a

^a Materials and Engineering Research Institute, Sheffield Hallam University,

Howarth St, Sheffield, UK.

Abstract. This note presents a novel scheme for modeling of reinforced concrete. The strategy takes into account the nonlinear behaviour of the concrete as well as the debonding in the interface. The proposed technique solves the kinematic and kinetic jump in the interface by performing sub-cycles over the constituents –reinforcing bar and concrete– jointly with an innovative interface constitutive law. Application to pull-out problems is performed to show the capabilities of the proposed methodology by means of comparison with available experimental data.

Keywords: reinforced concrete; debonding; interface law; finite elements

1 INTRODUCTION

The computer modeling of reinforced concrete remains a key issue due to the nonlinearity of the material components and the structural discontinuity that takes place in the interface. The concrete constitutive behaviour is non-linear due to its softening response after damage initiation. Thus, a return mapping algorithm (1, 2) is required to solve when using Newton-Raphson method or Arc-length methods, amongst other implicit schemes. Moreover, the interface kinematic jump causes stability problems if sub-cycles of solution are performed between the concrete and the reinforcing bar – henceforth rebar. In order to avoid this undesirable effect, a perfect bond is assumed in the interface by a number of authors, see for example (3, 4, 5, 6). In this paper, an imperfect bond is assumed –i.e. relative displacement is allowed in the interface between both components of the reinforced concrete.

Distinct meshes for both reinforced concrete constituents are conducted jointed by means of interface conditions. There have been a number of works dealing with mesh partitioning, e.g. (7, 8), or (9) for a comprehensive review. However, none of them is concerned about modeling of reinforced concrete. The proposed numerical procedure is based on sub-cycles of solution over the two constituents. Furthermore, governing equations for both compo-

nents are solved independently but including interface forces and interface boundary conditions that contains the interaction information with the other constituent.

This note is structured as follows. Firstly, a description of the implicit scheme used in the concrete sub-cycle of solution is presented. Secondly, the modeling of the interface containing the constitutive law. Thirdly, the explicit finite element method for rebars. Fourthly, application to pullout tests and comparison with experiments. Finally, conclusions arisen from this study are provided. To the author's knowledge, the proposed technique has not previously been considered.

2 MODELING OF REINFORCED CONCRETE

The proposed scheme is based in subcycles of solution over both constituents rebar and concrete with an innovative treatment of the interfacial forces within the governing equations. A so-called cycle in the reinforced concrete involves one sub-cycle in the concrete and another one in the rebar. A cycle may be seen as a global iteration. A number of cycles are needed to solve the whole mechanical problem to the required accurateness. The concrete

sub-cycle is solved by a standard implicit numerical method. In the interface, the kinematic jump is described by the relative displacement between rebar and surrounding concrete. The interface constitutive law provides the bond stress given a relative displacement. The interface forces are computed from the bond stress. They are considered external forces for the corresponding sub-cycle either in the concrete or in the rebar. The rebars are solved by an explicit numerical strategy. Henceforth, I superscript refers to the implicit scheme adopted for the concrete. Likewise, E superscript is associated to variables and parameters corresponding to the explicit strategy used for the rebar. The reinforced concrete physical domain is composed by the concrete sub-domain Ω and the rebar sub-domain Λ .

Implicit procedure for concrete

The finite element discretisation of the concrete domain Ω results in a system of algebraic equations representing equilibrium of momentum, Eq.(1). The residual \mathbf{R} is defined as the difference between internal forces $\mathbf{f}^{(int)I}(\mathbf{u}_{n+1}^I)$ and, external forces $\mathbf{f}_{n+1}^{(ext)I}$ and interface forces \mathbf{f}^{EI} . The latter one depends nonlinearly upon the relative displacements of concrete \mathbf{u}_{n+1}^I and rebar \mathbf{u}_n^E through the interface constitutive law.

$$\mathbf{R}(\mathbf{u}_{n+1}^I) := [\mathbf{f}^{(int)I}(\mathbf{u}_{n+1}^I)] - [\mathbf{f}_{n+1}^{(ext)I} + \mathbf{f}^{EI}(\mathbf{u}_{n+1}^I, \mathbf{u}_n^E)] \quad (1)$$

where $n + 1$ denotes the current cycle. \mathbf{u}_{n+1}^I are the displacements of the nodes of the concrete mesh domain and \mathbf{u}_n^E are the solution displacements of the rebar nodes at the former cycle.

The nodal internal force vector is written in Eq.(2). The integral is approximated by numerical integration as usual at quadrature points. The external force vector is defined in Eq.(3).

$$\mathbf{f}^{(int)I}(\mathbf{u}_{n+1}^I) = \bigwedge_{e=1}^{nelem} \left[\int_{\Omega^{(e)}} \mathbf{B}^T \boldsymbol{\sigma}(\boldsymbol{\varpi}_{n+1}^I, \boldsymbol{\varepsilon}_{n+1}^I) d\Omega \right] \quad (2)$$

$$\mathbf{f}^{(ext)I} = \bigwedge_{e=1}^{nelem} \left[\int_{\Omega^{(e)}} \mathbf{N}^T \mathbf{b} d\Omega + \int_{\partial\Omega^{(e)}} \mathbf{N}^T \mathbf{t} d\Gamma \right] \quad (3)$$

where $\bigwedge_{e=1}^{nelem}$ denotes the assembly operator, \mathbf{N} is the shape functions tensor, \mathbf{b} are the body forces, \mathbf{t} the traction forces applied over the boundary of the concrete domain. Note that the boundary of concrete $\partial\Omega$ does not include the interface with the rebar. \mathbf{B} is the linear strains operator, and $\boldsymbol{\sigma}$ the stress which depends upon the strains $\boldsymbol{\varepsilon}_{n+1}^I$ and internal variables $\boldsymbol{\varpi}_{n+1}^I$.

This system of equations Eq.(1) is linearised in order to accomplish a Newton-Raphson procedure, see (10) amongst others. The nonlinear material model used for concrete requires a return mapping algorithm for the

integration of the stress and internal variables. Thus, if a set of internal variables ϖ_n^I are given at sub-cycle n , then, the strain $\boldsymbol{\varepsilon}_{n+1}^I$ determines stresses $\boldsymbol{\sigma}_{n+1}^I$ only through integration algorithm. The interested reader is referred to textbooks (1, 2) for a comprehensive review of return mapping algorithms. It basically consists of an elastic trial prediction and, if yielding is reached, a plastic correction is performed subjected to consistency and softening –or hardening– constraints

The linearisation of Eq.(1) renders Eq.(4), see (10) for further details.

$$\mathbf{K}_T \delta \mathbf{u}^{I(k)} = -\mathbf{R}^{(k-1)}(\mathbf{u}_{n+1}^I) \quad (4)$$

where (k) is the current Newton-Raphson iteration, \mathbf{u}_{n+1}^I denotes the displacement at cycle $n + 1$, $\delta \mathbf{u}^{I(k)}$ is the unknown displacement increment vector at Newton-Raphson iteration (k) and \mathbf{K}_T is the global tangent stiffness matrix, Eq.(5).

$$\mathbf{K}_T = \left. \frac{\partial \mathbf{R}}{\partial \mathbf{u}^I} \right|_{\mathbf{u}_{n+1}^{I(k-1)}} \quad (5)$$

\mathbf{K}_T is obtained by assembly the element stiffness second-order tensors given at Eq.(6).

$$\mathbf{k}_T^{(e)} = \sum_{\xi=1}^{n_{gaus}} \omega_{\xi} \mathbf{B}_{\xi}^T \hat{\mathbf{D}}_{\xi} \mathbf{B}_{\xi} \quad (6)$$

where $\hat{\mathbf{D}}$ is the consistent tangent stiffness matrix, Eq.(7).

$$\hat{\mathbf{D}} = \frac{\partial \hat{\boldsymbol{\sigma}}}{\partial \boldsymbol{\varepsilon}_{n+1}} \Big|_{\boldsymbol{\varepsilon}_{n+1}^{(k-1)}} \quad (7)$$

2.1 Interface constitutive law

The connection of both sub-cycles is carried out in the interface. Equilibrium is reached at the interface after a number of cycles to the required accurateness. Element interface forces, Eq.(8), are defined as the bond stress multiplied by the corresponding perimetric area of the rebar element.

$$\mathbf{f}_e^{EI}(\mathbf{u}_{n+1}^I, \mathbf{u}_n^E) := \boldsymbol{\tau}[\mathbf{s}_{n+1}^{EI}(\mathbf{u}_{n+1}^I, \mathbf{u}_n^E)] A_e \quad (8)$$

Above, A_e is the perimetric area of the considered element e and $\boldsymbol{\tau}$ is the bond stress depending upon the slip \mathbf{s}_{n+1}^{EI} . The interface constitutive law is a functional that relates slip and bond stress. A generic component j of $\boldsymbol{\tau}$ is computed through the following interface law,

$$\tau_j(s) = \begin{cases} \alpha_1 K_{bond} \frac{s_j}{s_o} + \alpha_2 \tau_y \left(\beta_1 \frac{s_j}{s_o} + \beta_2 \left(\frac{s_j}{s_o} \right)^2 + \beta_3 \left(\frac{s_j}{s_o} \right)^3 \right), & \forall \left| \frac{s_j}{s_o} \right| < \delta^* \\ \text{sign}(s_j) \cdot \tau_y, & \forall \left| \frac{s_j}{s_o} \right| \geq \delta^* \end{cases}$$

where $K_{bond} = \tau_y/\delta^*$ and δ^* is the critical ratio for yielding which depends upon the type of interface. $\alpha_1, \alpha_2, \beta_1, \beta_2, \beta_3$ are interface parameters. The

slip –or relative displacement– is defined as the difference between displacements in concrete and rebar in an absolute value, Eq.(9).

$$\mathbf{s}_{n+1}^{EI}(\mathbf{u}_{n+1}^I, \mathbf{u}_n^E) = \mathbf{u}_{n+1}^I - \mathbf{u}_n^E \quad (9)$$

The proposed interface law is a functional of the relative displacements between adjacent elements. Thus, in the case of using other methods such as discrete element methods, the bond forces acting upon adjoining elements could be computed provided the relative displacement between these.

Other approaches such as cohesive zone models have been widely used in concrete modelling. This is mainly due to the easy integration within finite element method. A cohesive zone model is normally a relationship between traction and separation, mode I, ahead of the crack tip capable of macroscopically simulating crack growth. However, the proposed interface law has proved to be convenient when such a kinetic and kinematic jumps appear in the interface. This results in an adequate transmission of conditions in the interface without compromising the stability of the proposed numerical strategy. The cohesive zone model is normally used throughout the concrete and not in the interface with the steel re-bars, and no fracture is simulated in the concrete in this work. So, no attempt is done to modeling the concrete with any cohesive zone model at this time.

2.2 Explicit procedure for the rebars

The spatial discretisation by finite elements results in a system of second order differential momentum equations which results in the Eq. 10. These governing equations are solved by standard *Central Differences*.

$$\mathbf{M}^E \ddot{\mathbf{u}}^E(t_i) + \mathbf{C}^E \dot{\mathbf{u}}^E(t_i) + \mathbf{f}^{(int)E}(\mathbf{u}_i^E) = \mathbf{f}^{(ext)E} + \mathbf{f}^{IE}(\mathbf{u}_n^I, \mathbf{u}_n^E) \quad (10)$$

where \mathbf{M}^E is the mass matrix, \mathbf{C}^E is the damping matrix assumed proportional to the mass matrix, $\mathbf{f}^{(ext)E}$ are the external forces applied directly on the rebar. The rebar is modelled with continuum-based beam elements. Details of these elements may be found on reference (13). Note that, in general, external forces vanish if the rebar is embedded within the concrete.

Remark: In this study, only quasi-static problems are undertaken. The fact of that the inertia and damping terms appear in (10) is artificial and is used to perform an explicit scheme by dynamic relaxation. The static solution is obtained from the attenuation of the transient response, leaving the static solution for the applied load. Details of this technique are shown in (11).

COMPUTATIONAL ALGORITHM

The algorithm is resumed below,

- i Initiate Newton-Raphson iterations ($k=0$) for cycle $n + 1$ at concrete mesh domain.

$$\mathbf{u}_{n+1}^{I(0)} = \mathbf{u}_n^I$$

$$\mathbf{R} = \mathbf{f}^{(int)I}(\mathbf{u}_{n+1}^I) - \mathbf{f}_{n+1}^{(ext)I} - \mathbf{f}^{EI}(\mathbf{u}_{n+1}^I, \mathbf{u}_{n+1}^E)$$

- ii For all concrete finite elements, calculate the consistent tangent stiffness matrix (1),

$$\hat{\mathbf{D}} = \left. \frac{\partial \hat{\boldsymbol{\sigma}}}{\partial \boldsymbol{\varepsilon}_{n+1}} \right|_{\boldsymbol{\varepsilon}_{n+1}^{(k-1)}}$$

where $\hat{\boldsymbol{\sigma}}$ is the stress tensor obtained by means of the return mapping algorithm (1, 2).

- iii Element stiffness matrices

$$\mathbf{k}_T^{(e)} = \sum_{\xi=1}^{n_{gaus}} \omega_{\xi} \mathbf{B}_{\xi}^T \hat{\mathbf{D}}_{\xi} \mathbf{B}_{\xi}$$

where ω_{ξ} is the weight associated to the gauss point ξ .

- iv Increment iteration counter ($k=k+1$), assemble, solve the linearized equilibrium equation (4) and update stress tensor and internal variables

through integration algorithm (1),

$$\begin{aligned}\mathbf{u}_{n+1}^{I(k)} &= \mathbf{u}_{n+1}^{I(k-1)} + \delta \mathbf{u}^{I(k)} & \boldsymbol{\varepsilon}_{n+1}^{(k)} &= \mathbf{B} \mathbf{u}_{n+1}^{I(k)} \\ \boldsymbol{\sigma}_{n+1}^{(k)} &= \hat{\boldsymbol{\sigma}}(\boldsymbol{\varepsilon}_{n+1}^{(k)})\end{aligned}$$

vi Compute new internal forces at each element

$$\mathbf{f}_{(e)}^{I int} = \sum_{\xi=1}^{n_{gaus}} \xi_{\xi} J_{\xi} \mathbf{B}_{\xi}^T \boldsymbol{\sigma}_{n+1, \xi}^{(k)}$$

vii Assemble element internal forces vector and update residual.

viii (a) If

$$\frac{\|\mathbf{f}_{n+1}^{(ext) I} + \mathbf{f}^{EI}(\mathbf{u}_{n+1}^I, \mathbf{u}_n^E) - \mathbf{f}^{(int) I}(\mathbf{u}_{n+1}^{I(k)})\|}{\|\mathbf{f}_{n+1}^{(ext) I} + \mathbf{f}^{EI}(\mathbf{u}_{n+1}^I, \mathbf{u}_n^E)\|} \leq \epsilon \quad (11)$$

then solution for current external load is reached and values for this sub-cycle are from Newton-Raphson iteration (k) , $(\bullet)_{n+1} = (\bullet)_{n+1}^{(k)}$. ϵ is the tolerance establishing the level of accurateness required.

Start explicit scheme in the other partition for the current cycle.

The initiation at $t_0 = t(i = 0)$, i.e. initiation of a sub-cycle in a rebar, of the explicit marching scheme is performed as follows,

$$\dot{\mathbf{u}}_{\frac{1}{2}}^E = \mathbf{M}^E (\mathbf{f}^{(ext) E} + \mathbf{f}^{IE}(\mathbf{u}_n^I, \mathbf{u}_n^E) - \mathbf{f}^{(int) E}(t_0)) \frac{\Delta t_1}{2}$$

$$\mathbf{u}_0^E = \mathbf{u}_n^I ; \quad \mathbf{u}_1^E = \mathbf{u}_0^E + \Delta t_{\frac{1}{2}} \dot{\mathbf{u}}_{\frac{1}{2}}^E$$

Note that \mathbf{u}_n^I denotes the prescribed displacements only for the nodes within the interface. The following steps at a generic $t_i \in \mathbb{R}_+$ is conducted by,

$$(2\mathbf{M}^E + \Delta t_i \mathbf{C}^E) \cdot \dot{\mathbf{u}}_{i+\frac{1}{2}}^E = (2\mathbf{M}^E - \Delta t_i \mathbf{C}^E) \cdot \dot{\mathbf{u}}_{i-\frac{1}{2}}^E + \mathbf{f}^{(ext)E} + \mathbf{f}^{IE}(\mathbf{u}_n^I, \mathbf{u}_n^E) - \mathbf{f}^{(int)E}(t_i) \quad (12)$$

$$\mathbf{u}_{i+1}^E = \mathbf{u}_i^E + \Delta t_{i+\frac{1}{2}} \dot{\mathbf{u}}_{i+\frac{1}{2}}^E$$

The system (12) becomes a set of uncoupled set of algebraic equations as \mathbf{M}^E and \mathbf{C}^E are chosen diagonal, see (12) for definition of these matrices.

(b) else go to (ii).

ix If the total load is not completely applied, increment external load and go to (ii).

3 NUMERICAL EXAMPLE

The pull-out test is a key example to analyse the interaction in the interface. Basically, it consists of a reinforcing bar which is pulled out from the concrete. Rebar nodes are initially coincident in the same spatial position with the

concrete nodes in the interface. Bond stress increases, according to the law presented above, with the slip in the interface. The slip is mainly due to stretching of the rebar. The concrete nodes in the boundary (except those on the side in which the free edge of the bar is located) are constrained Figure 1.

The concrete is modelled, by quadratic quadrilaterals, as a material in which friction and dilatancy angles coincide (20°). The other parameters needed for concrete are: Young modulus 14 GPa , Poisson ratio 0.1, yield stress in compression 30.5 MPa and yield stress in tension 2.75 MPa . The rebar is modelled by continuum-based beam elements (13) with a cross-section area of $\pi \cdot 10^2\text{ mm}^2$ and an embedded length of 350 mm . The rebar is assumed elastic-plastic with Young modulus 180 GPa , Poisson ratio 0.33 and yield stress 300 MPa . The reinforced concrete is such that the slip for yielding is $s_o = 0.6\text{ mm}$ ($\delta^* = 1$) and the yield bond stress is $\tau_y = 8\text{ MPa}$, (14, 15). The parameters of the interface law were set –after calibration for the given reinforced concrete– to: $\alpha_1 = 0.2$, $\alpha_2 = 0.1$, $\beta_1 = 5$, $\beta_2 = -4.5$, $\beta_3 = 1.4$. A two-dimensional plane stress problem with a thickness of 78.5 mm is assumed. These data are consistent with the specimen used by Farmer (16) in his pullout experiments. In these experiments, the rebar was instrumented

with eight strain gauges in axial direction in the experiments to be able of measuring strains in the interface.

The bar is loaded incrementally with a longitudinal force up to 100 KN which leads to yielding in some parts of the interface, i.e. the maximum bond stress is reached, see Figure 2. The behaviour of bond stress along the bar is non-linear as can be observed in Figure (3). It is observed that the slip is sufficient to yield -8 MPa near of the loaded edge. In Figure (3) is observed good agreement with the experimental results by Farmer (16) in most of the length of the rebar. However, there is disagreement in the inner part. This is due to the assumption of the inner end of the rebar completely fixed which is a very strict constraint. The main reason is that the interior edge node is constrained in displacement for stability reasons. In a real set-up this is not the case. That is causing this mismatch of bond stress close to the interior edge node for smaller values of x , see Figure (3).

4 CONCLUSIONS

This note presented an innovative scheme to undertake the modeling of reinforced concrete. It makes use of properly modified standard numerical

procedures to take into account the kinematics and kinetics of the interface. The strategy permits to take into account the nonlinear behaviour of the concrete as well as the slip between rebars and the concrete. Within this approach, two main advantages may be highlighted. Firstly, efficiency to deal with the discontinuity in the interface avoiding instability and, hence, divergence of the numerical procedure. This is mainly due to that the kinematic jump in the interface between both material components is avoided. Also, the interface conditions are conveniently addressed in the governing equations of both material. Interface forces were introduced as external forces for the correspondent material constituent. Secondly, computational cost is reduced thanks to the use of different time integrators for each material component. However, it should be stated that this saving is an advantage only when dealing with very restricted stability conditions. Otherwise, a simple direct integration over a partitioned mesh could be more convenient due to the number of cycles conducted –in the proposed scheme– for convergence to a required accurateness. Details of its implementation within an *in-house* finite element code were presented as well as key numerical tests.

References

- [1] J. C. Simo and T. J. R. Hughes. *Computational Inelasticity*. Springer-Verlag, New York, 1998.
- [2] E. A. de Souza Neto, D. Peric, and D. R. J. Owen. *Computational Methods for Plasticity: Theory and Applications*. Wiley Blackwell, Chichester, UK, 1st edition, 2008.
- [3] H. G. Kwak and F. C. Filippou. Nonlinear fe analysis of r/c structures under monotonic loads. *Computers and Structures* 1997; 65(1):1–16.
- [4] I. M. May, C. T. Morley, and Y. Y. Chen. Benchmarking of non-linear finite element analyses for reinforced concrete deep beams. In N. Bicanic, R. de Borst, H. Mang, and G. Meschke, editors, *Proc. Euro-C, Conf. Computational Modeling of Concrete Structures*, Mayrhofen, Tyrol, Austria, 2003. A A Balkema Publishers..
- [5] S. Teng, Y. Liu, and C. K. Soh. Analysis of concrete slabs using shell element with assumed strain. *ACI Structural Journal* 2005; 102(4):515–524.
- [6] Y. X. Zhang, M. A. Bradford, and R. I. Gilbert. A new triangular

- layered plate element for the non-linear analysis of reinforced concrete slabs. *Commun. Numer. Meth. Engng* 2006; 22(7):699–709.
- [7] T. J. R. Hughes and W. K. Liu. Implicit-explicit finite elements in transient analysis: implementation and numerical examples. *Journal of Applied Mechanics* 1978; 45:375–378.
- [8] T. Belytschko and R. Mullen. Stability of explicit-implicit mesh partitions in time integration. *Int. J. Numer. Meth. Engng.* 1978; 12:1575–1586.
- [9] C. A. Felippa, K. C. Park, and C. Farhat. Partitioned analysis of coupled mechanical systems. *Comput. Methods Appl. Mech. Engrg.* 2001; 190:3247–3270.
- [10] J. Bonet and R. D. Wood. *Nonlinear Continuum Mechanics for Finite Element Analysis*. Cambridge University Press, 1997.
- [11] T. Belytschko and T.J.R. Hughes, editors. *Computational Methods for Transient Analysis*, The Netherlands, 2001. Elsevier Science B.V.
- [12] J. L. Curiel Sosa, E. A. de Souza Neto, and D. R. J. Owen. A combined

implicit-explicit algorithm in time for non-linear finite element analysis.

Commun. Numer. Meth. Engng 2006; 22:63–75.

- [13] J.L. Curiel Sosa and A.J. Gil. Analysis of a continuum-based beam element in the framework of explicit fem. *Finite Elements in Analysis and Design* 2009; 45:583–591.

- [14] L. J. Sluys and R. de Borst. Failure in plain and reinforced concrete-an analysis of crack width and crack spacing. *Int. J. Solids Structures* 1996; 33(20-22):3267–3276.

- [15] D. Roberts. *Finite Element Modeling of Rockbolts and Reinforcing Elements*. Phd thesis, University of Wales Swansea, Swansea, 1999.

- [16] I. W. Farmer. Stress distribution along a resin grouted rock anchor. *Int. J. Rock Mech. Min. Sci. Geomech.* 1975; 12:347–351.

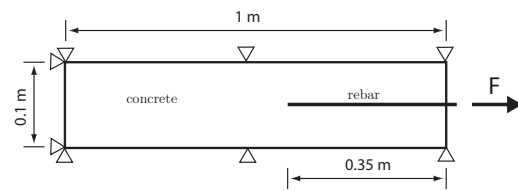


Figure 1: Details of the idealised configuration of the pullout test in a two-dimensional context

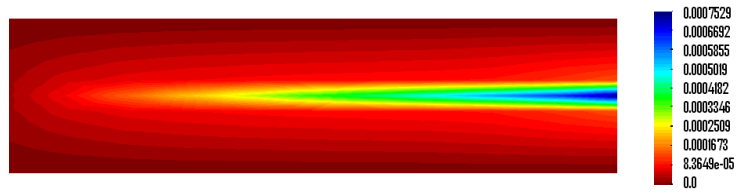


Figure 2: Displacement field contours (m) -only half of the sample is depicted- in the concrete. Displacements of the rebar nodes are not represented.

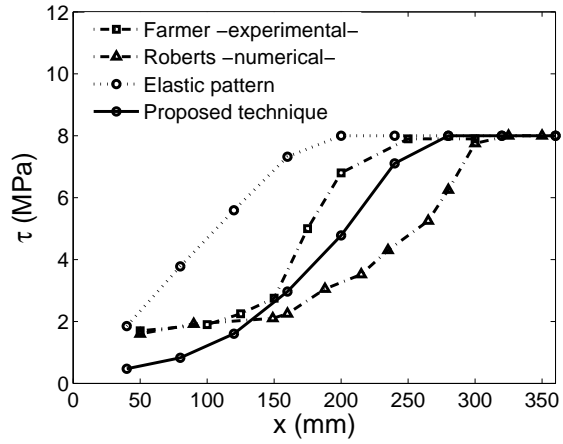


Figure 3: Numerical versus experimental bond stress along the reinforcement. External force = 100 *KN*. Elastic pattern refers to an elastic interface law assumption and it is provided for comparison purposes with the more realistic proposed law.